

MODELLING SUPERNOVA RADIO EMISSION: OUR FIRST STEPS

M. Orellana^{1,2} and M. Bersten³

RESUMEN

Las supernovas (SNs) son poderosas explosiones estelares que marcan la etapa final en la evolución de algunas estrellas. Son eventos extremadamente luminosos que se pueden detectar a distancias cosmológicas. Su estudio tiene una intrincada conexión con varios problemas astrofísicos y, por lo tanto, han merecido grandes inversiones en términos de campañas de observación. Los estudiamos desde una perspectiva complementaria: tratamos de explicar las observaciones ópticas derivando las propiedades físicas de las explosiones y los progenitores estelares. Después de aplicar un código hidrodinámico 1D que propaga la radiación y cuenta con una larga historia de resultados ya publicados, podemos estimar la emisión térmica que se canaliza a longitudes de onda de radio. Como han encontrado otros estudios, dicha componente no es suficiente para explicar la mayoría de las SNs observadas que han sido monitoreadas hasta ahora por diferentes radiotelescopios. Para comprender la emisión de radio, la interacción con el material circunestelar parece ser muy relevante. Nuestras perspectivas, en un futuro cercano, son desarrollar cálculos que proporcionen luminosidades no térmicas que nuestro código no estima actualmente. Con base en la literatura y experiencias propias, discutimos qué tipo de suposiciones se necesitan para lograr ese objetivo. Nuestro enfoque estará dirigido a la emisión que producen las explosiones de supernovas en el rango de energía de baja frecuencia (100 MHz - 2 GHz) propuesto para las futuras instalaciones que operarán en nuestro país.

ABSTRACT

Supernovae (SNe) are powerful stellar explosions that mark the final stage in the evolution of some stars. They are extremely luminous events that can be detected out to cosmological distances. Their study has an intricate connection with various astrophysical topics, and therefore they have deserved large investments in terms of observational campaigns. We study them from a complementary perspective, trying to explain optical observations by deriving the physical properties of the explosions and the stellar progenitors. After applying a 1D radiation-hydrodynamic code with a long history of results already published, we can estimate the thermal emission that is channeled to radio wavelengths. As found by other studies, this component is not enough to explain most of the observed SNe that have been monitored so far by different radio telescopes. In order to understand radio emission, interaction with circumstellar material seems to be very relevant. Our prospects, in the near future, are to develop calculations that provide non-thermal luminosities that our code does not currently estimate. Based on the literature and our experience, we discuss what kind of assumptions are needed to achieve that goal. Our focus will be directed to the emission produced by supernovae explosions at the low-frequency energy range (100 MHz - 2 GHz) proposed for future facilities that will operate in our country.

Key Words: Numerical simulations — Radiative processes — Radioastronomy — Supernovae: general

1. INTRODUCTION: THE TIME DEPENDENT RADIO LANDSCAPE

A large number of radio emitting transients have been recorded, including extragalactic SNe, gamma-ray bursts, and tidal disruption events among other

more faster phenomena. A substantial collection of light curves (LCs) was compiled by Mooley et al. (2022), as well as other analysis showing the luminosity vs. timescale and the energy vs. blastwave mean velocity. This illustrate a growing landscape where radio spectral luminosities range from $10^{25} - 10^{32}$ erg s⁻¹ Hz⁻¹ for 1–5 GHz frequencies. We will focus here on core collapse SNe, the destruction of massive stars. Our final goal is to predict their radio emission. Our job is in preliminary state.

The best studied case of a radio-loud supernova is SN1993J (e.g. Weiler et al. 2007, Marcaide et al.

¹Universidad Nacional de Río Negro. Laboratorio de Investigación Científica en Astronomía (LICA, CITECCA), Sede Andina, Mitre 630 (8400) Bariloche, Argentina (morellana@unrn.edu.ar).

²Consejo Nacional de Investigaciones Científicas y Técnicas (CONICET), Argentina.

³Instituto de Astrofísica de La Plata (IALP), CCT-CONICET-UNLP. Paseo del Bosque S/N (B1900FWA), La Plata, Argentina.

2009). Very few so bright and close SNe are resolved through Very Long Baseline Interferometry. In this outstanding case the SN was followed during the slow-down to around 30% of its original expansion velocity. Nowadays is gently transitioning to a SN Remnant. Latest reported data are into the midIR domain and were found in the archival of Spitzer 26 yr post-explosion (Zsíros et al. 2022).

At a distance of $d = 3.64$ Mpc, SN1993J holds an excellent subject for a comprehensive theoretical-observational analysis. Efforts in this sense were done by Fransson & Björnsson (1998). Within a similar classification (SNe IIf/Ib/Ic/IIn/IIL, Filippenko 1997 for the spectral and photometric subclasses) there are other detections of young supernovae, i.e. ~ 1 year after the explosion, at radio wavelengths, and at X-rays in some cases (e.g. Chandra et al. 2012, Chevalier & Fransson 2017, Ho et al. 2022). An updated picture of the population of radio SNe can be drawn from the sample compiled from the literature by Bietenholz et al. (2021), containing a comprehensive set of 2–10 GHz radio flux density measurements and upper limits of 294 SNe. Around 31% of the sample are detected SNe, and the typical maximum radio fluxes of the order of ~ 1 mJy are close to the sensitivity limits of present detectors. The radio LCs of SNe are found to be extremely varied.

2. TWO SNE THAT WE HAVE STUDIED

In relation with studies that we have conducted, we mention the extensive radio monitoring of SN 2016gkg, during $t \sim 8 - 1429$ days post-explosion, reported by Nayana et al. (2022). The authors found the radio light curves and spectra are broadly consistent with self-absorbed synchrotron emission. In Bersten et al. (2018) we reported and analysed optical data of this SN: the cadence of the initial observations allowed us to study in detail the outermost structure of the progenitor of the supernova and the physics of the emergence of the shock. In order to reproduce the fast post-shock cooling peak, an extended H-rich envelope has to be attached to the usual progenitor structure from stellar-evolution calculations (provided by Nomoto & Hashimoto 1988 in our case). For the extended envelope we found a radius of $R_{\text{env}} \approx 320 R_{\odot}$ and a mass of $M_{\text{env}} \simeq 0.02 M_{\odot}$ as depicted in Section 4. Later observations provided new constraints and debated the stellar progenitor radius (Kilpatrick et al. 2022). Note the posterior radio study by Nayana et al. (2022) provides an independent tool for exploring the mechanism of the stellar mass loss prior to

the explosion, which is strongly related to the pre-supernova evolution.

Previously we have studied the SuperLuminous SN (SLSN) ASASSN-15lh. Given its peak luminosity and early-time spectra, this was mentioned as the most luminous supernova ever discovered⁴. In Bersten et al. (2016) we found that is physically plausible to reproduce the overall shape of the LC through the presence of a central magnetar that loses rotational energy. At Fig. 1 we compare the bolometric data of the mentioned SNe along with our preferred models for the LCs. Data were taken from our publication of SN2016gkg and from Godoy-Rivera et al. (2017) in the case of ASASSN-15lh.

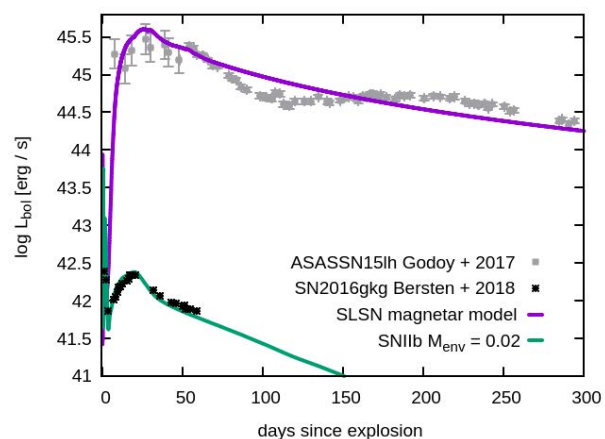


Fig. 1. Examples of bolometric light curves computed with our code. The normal type IIf corresponds to SN2016gkg, and the SLSN to ASASSN-15lh.

3. METHODS

We used a one-dimensional local thermal equilibrium hydrodynamical code (Bersten et al. 2011) to perform the numerical calculations. The code assumes the diffusion approximation for optical photons. The formation of the shock wave following core collapse is started by artificially adding internal energy (thermal bomb). For the γ -rays produced through the radioactive decay of the ^{56}Ni -chain, a gray approximation is applied. From the crude treatment of the radiation transfer, and by assuming a black body emission, the broadband photometry can be estimated. In radio, the detectable flux is also regulated by the frequency bandwidth, and we have to be sure of which temperature is correct for the

⁴Though there are other ideas, like the tidal disruption event, presented by Mummery & Balbus (2020), or a massive ejecta shocking a very strong wind ejected by the progenitor star before the explosion (Huang & Li 2018), or combined power inputs (Chatzopoulos et al. 2016).

computation of outgoing photons. In Fig. 2 we show the evolution of the thermalization temperature and the photospheric temperature.

We follow the evolution of the LC in a self consistent way up to the nebular phase, therefore, in the following we decided to present the results during the epochs when the approximations are realistic. For illustration we compare the mentioned SNe but they are clearly quite different, not only in the visual range, but since in the case of ASASSN-15lh no radio emission was detected, to an upper limit of 23 microJy using ATCA (Kool et al. 2015). In addition, the distance of the host galaxy is ~ 1171 Mpc, much larger than the ~ 26.6 Mpc of SN2016gkg.

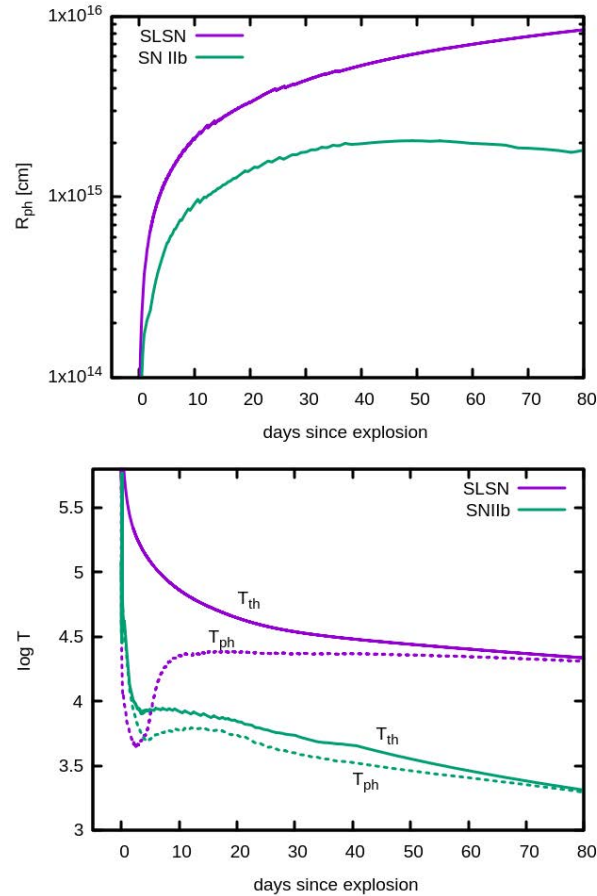


Fig. 2. Most relevant output computed with our code that can be used for a crude estimation of the black body emission at a desired wavelength or band. *Top panel:* The photospheric radius as a function of time. *Bottom panel:* characteristic temperatures, at thermalization condition and at the optical photosphere. See Bersten et al. (2011) for the details.

In Fig. 3 we show the calculated thermal emission for the SNe we have previously modeled, but now channelled to radio wavelengths. We set an

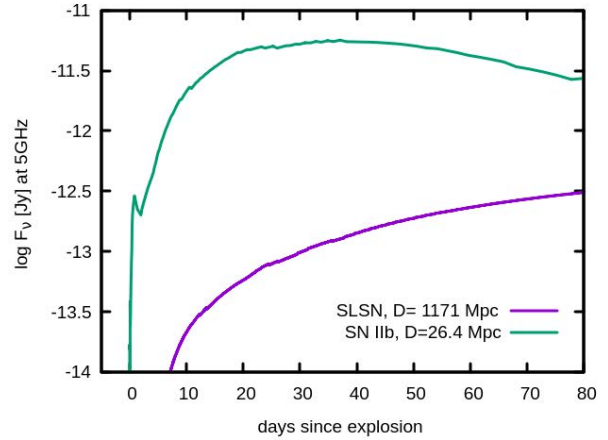


Fig. 3. Thermal emission flux that is channelled to radio wavelengths. This component is not enough to explain the observed radio LC of the ordinary type IIb SN2016gkg but does not contradict the non-detection of the SLSN ASASSN-15lh.

artificial radio band centered at 5 GHz, comparable with the one in many of the mentioned works. The resulting component of radio flux is rather too small, below any possible chance for detection with actual instruments. It will also be under the capabilities for the low-frequency energy range 100 MHz - 2 GHz, and deserves further investigation including the non-thermal emission. If the signal is strong, splitting the total bandwidth into spectral windows is normally desirable. Note that SLSNe examples not as extreme as ASASSN-15lh have been detected in radio (e.g. SN 2017ens, Chen et al. 2018).

4. SN INTERACTING WITH SURROUNDING MATTER

From the observed radio spectra and LC, the radio loud supernova SN2016gkg (Nayana et al. 2022) provides an example of a shock that reach the conditions for particle acceleration and then, the radiative processes that dominate the radio emission are of non-thermal kind (Ginzburg & Syrovatskii 1964), being synchrotron or free-free the more effective at the \sim GHz band. Radio absorption parameters are also considered: below a turn-over frequency the source is expected to become optically thick.

The presence of matter at the outskirts of the star is therefore decisive. That was long ago established by the study of Chevalier (1982) and improvements afterwards. A standard, parametric model of the radio emission from a SN interacting with circumstellar matter (CSM) assumes the blastwave velocity, v_{sh} and two important values: the fraction ϵ_e of the

energy transferred to the nonthermal electrons and ϵ_B , the amplification efficiency. Then these relations hold

$$u_e = \epsilon_e \rho_{\text{sh}} v_{\text{sh}}^2 \quad (1)$$

for the high-energy particles total budget, here assumed to be electrons, and

$$B = (8\pi\epsilon_B\rho_{\text{sh}}v_{\text{sh}}^2)^{1/2} \quad (2)$$

for the magnetic field strength. The time dependence enters through $r \propto t^m$ with an expansion index m , the density of the CSM is assumed to follow $\rho_{\text{CMS}} \propto r^{-s}$, where the ejecta follows $\rho_{\text{ej}} \propto r^{-n}$. Usually the CSM density profile is set to $\propto r^{-2}$. The index n for the ejecta can be obtained from the simulations, or many authors use it as a free parameter.

Not uniform mass loss from the progenitor (see Lamers & Cassinelli 1999) can be invoked whenever the s index changes, because it means the shock has reached a shell of slower material. In other words, radio emission comes not only from the interaction between the supernova ejecta and the immediate CSM, but is also possible that an external shell of the dying star is located further and radiates later as the explosion’s forward shock expands in the medium previously sculpted by the mass-loss history of the stellar progenitor (DeMarchi et al. 2022).

An advancing overdensity is recovered by our simulations as illustrated in Fig. 5. A stellar envelope is piled and compressed by the shock front of the SN. The usual parameters for the initial density profile are the mass loss rate \dot{M} , the external radius R , and terminal velocity, along with the radial profile dependence of the envelope velocity, which is a power law for simplicity. The ambient medium may have other configurations, signed by clumps or anisotropies. It should be also noticed that our 1D approach is unable to properly catch Rayleigh-Taylor instabilities that occur behind the shock front, as obtained in multi-dimensional hydrodynamic calculations and supported by observations. This and other kind of instabilities are relevant for the magnetic field amplification and efficient cosmic ray acceleration (see also Maeda 2013).

5. WORK IN PROGRESS AND OBSERVATIONAL NOTES

One leading path to our research is provided by Matsuoka et al. (2019) who already related hydrodynamic simulations and non-thermal calculations. The methods of study for a density jump in other context like i.e. novae (del Valle et al. 2022) are also a guide that we shall consider.

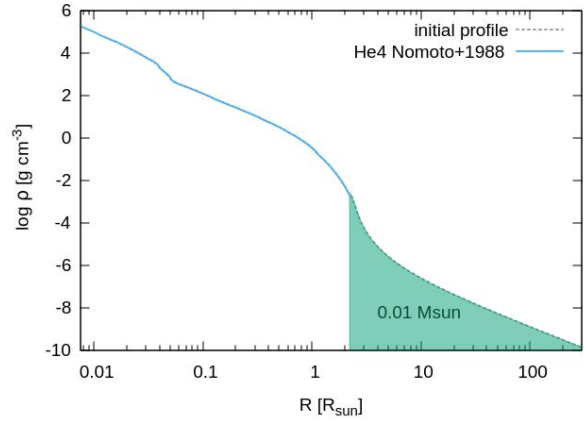


Fig. 4. Stellar density profile before SN explosion with an attached envelope of low mass. This is normally prescribed for type IIb explosions.

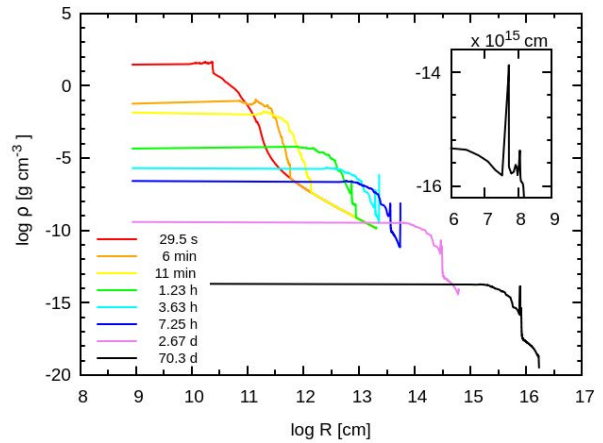


Fig. 5. Changes in the density profile as a function of interior mass during the shock propagation. An overdense shell or contact discontinuity is formed. Although we can not treat properly the instabilities that likely occur behind the shock, we gain a rough estimation of the shell where particle acceleration and magnetic field amplification should take place.

The stated hypothesis regarding magnetic field amplification and particle acceleration, that our code cannot compute at the moment, need to be added in the more consistent possible way. Our expectation is to have a parametric postprocessing of the hydrodynamic output in the near future. So it is possible to predict phenomenology at different wavelengths (beyond radio), and the CSM properties could be tested in order to contrast with other references. For instance, it has become of great interest to explore the millimeter wavelengths since there are new follow-up of SNe at this range (see Maeda et al. 2023) using

ALMA. We wonder if the future Large Latin American Millimeter Array (LLAMA) would get involved in this kind of projects. Emerging collaborations could be of interest. In that sense, we expect to count in Argentina with different facilities and improving technologies for the general advance of radioastronomy. We think it is promising as a science case to acquire the ability for rapid follow-up observations of SNe in the radio domain. An expert on the matter pointed us (personal communication) that radio time on SNe is getting difficult with the interferometric arrays. With single dish, there are potential issues due to contamination by the host galaxy and poor resolution, plus the factor of sensitivity, but the perspective improves if we were lucky to have a nearby SN explosion, or interesting afterglow as GRB221009A (Sato et al. 2023). An optimized radio follow-up strategy for core-collapse SNe was proposed by Carbone & Corsi (2020), perhaps we are at a propitious moment to revise its local applicability. At the other extreme of the electromagnetic spectrum, the High Energy Stereoscopic System dedicates target of opportunity time for the search of early very-high-energy γ -ray emission towards nearby core-collapse supernovae and supernova candidates, up to ~ 10 Mpc, within a few weeks after discovery (Hess et al. 2022). A successful detection could be of interest of the theoretical researchers of the *Instituto Argentino de Radioastronomía* who have a long history of modelling gamma-ray sources.

Acknowledgements: M.O. thanks the workshop organizers for the financial support and congratulates on the successful and cordial meeting held on the occasion of the IAR anniversary. This research was partially fund by UNRN PI2020 40B885.

REFERENCES

- Bersten, M. C., Benvenuto, O., & Hamuy, M. 2011, *ApJ*, 729, 61
- Bersten, M. C., Benvenuto, O. G., Orellana, M., et al. 2016, *ApJ*, 817, L8
- Bersten, M. C., Folatelli, G., García, F., et al. 2018, *Nature*, 554, 497
- Bietenholz, M. F., Bartel, N., Argo, M., et al. 2021, *ApJ*, 908, 75
- Carbone, D. & Corsi, A. 2020, *ApJ*, 889, 36
- Chandra, P., Chevalier, R. A., Chugai, N., et al. 2012, *ApJ*, 755, 110
- Chatzopoulos, E., Wheeler, J. C., Vinko, J., et al. 2016, *ApJ*, 828, 94
- Chen, T.-W., Inserra, C., Fraser, M., et al. 2018, *ApJ*, 867, L31
- Chevalier, R. A. 1982, *ApJ*, 259, 302
- Chevalier, R. A. & Fransson, C. 2017, *Handbook of Supernovae*, 875
- del Valle, M. V., Araudo, A., & Suzuki-Vidal, F. 2022, *A&A*, 660, A104
- DeMarchi, L., Margutti, R., Dittman, J., et al. 2022, *ApJ*, 938, 84
- Filippenko, A. V. 1997, *ARA&A*, 35, 309
- Fransson, C. & Björnsson, C.-I. 1998, *ApJ*, 509, 861
- Ginzburg, V. L. & Syrovatskii S. I. 1964, *The Origin of Cosmic Rays*, Pergamon Press, New York
- Godoy-Rivera, D., Stanek, K. Z., Kochanek, C. S., et al. 2017, *MNRAS*, 466, 1428
- Hess, Abdalla, H., Aharonian, F., et al. 2022, 37th International Cosmic Ray Conference, 809
- Ho, A. Y. Q., Margalit, B., Bremer, M., et al. 2022, *ApJ*, 932, 116
- Jin, H., Yoon, S.-C., & Blinnikov, S. 2021, *ApJ*, 910, 68
- Huang, Y. & Li, Z. 2018, *ApJ*, 859, 123
- Kilpatrick, C. D. et al. 2022, *ApJ*, 936, 111
- Kool, E. C., Ryder, S. D., Stockdale, C. J., et al. 2015, *The Astronomer's Telegram*, 8388
- Lamers, H. J. G. L. M. & Cassinelli, J. P. 1999, *Introduction to Stellar Winds*, Cambridge University Press, Cambridge
- Leung, J. K., Murphy, T., Ghirlanda, G., et al. 2021, *MNRAS*, 503, 1847
- Maeda, K. 2013, *ApJ*, 762, L24
- Maeda, K., Michiyama, T., Chandra, P., et al. 2023, *ApJ*, 945, L3
- Marcaide, J. M., Martí-Vidal, I., Alberdi, A., et al. 2009, *A&A*, 505, 927
- Matsuoka, T., Maeda, K., Lee, S.-H., et al. 2019, *ApJ*, 885, 41
- Mooley, K. P., Margalit, B., Law, C. J., et al. 2022, *ApJ*, 924, 16
- Mummery, A. & Balbus, S. A. 2020, *MNRAS*, 497, L13
- Nayana, A. J., Chandra, P., Krishna, A., et al. 2022, *ApJ*, 934, 186
- Nomoto, K. & Hashimoto, M. 1988, *Phys. Rep.*, 163, 13
- Sato, Y., Murase, K., Ohira, Y., et al. 2023, *MNRAS*, 522, L56
- Stroh, M. C., Terreran, G., Coppejans, D. L., et al. 2021, *ApJ*, 923, L24
- Weiler, K. W., Williams, C. L., Panagia, N., et al. 2007, *ApJ*, 671, 1959
- Zsíros, S., Nagy, A. P., & Szalai, T. 2022, *MNRAS*, 509, 3235